Breast Cancer Research

Breast Cancer RESEARCH

Optical imaging correlates with magnetic resonance imaging breast density and reveals composition changes during neoadjuvant chemotherapy

Breast Cancer Research 2013, **15**:R14 doi:10.1186/bcr3389

Thomas D O'Sullivan (tosulliv@uci.edu)
Anais Leproux (aleproux@uci.edu)
Jeon-Hor Chen (jeonhc@uci.edu)
Shadfar Bahri (sbahri@uci.edu)
Alex Matlock (amatlock@uci.edu)
Darren Roblyer (roblyer@bu.edu)
Christine E McLaren (cmclaren@uci.edu)
Wen-Pin Chen (wenpinc@uci.edu)
Albert E Cerussi (acerussi@uci.edu)
Min-Ying Su (msu@uci.edu)
Bruce J Tromberg (bjtrombe@uci.edu)

ISSN 1465-5411

Article type Research article

Submission date 1 October 2012

Acceptance date 14 February 2013

Publication date 22 February 2013

Article URL http://breast-cancer-research.com/content/15/1/R14

Optical imaging correlates with magnetic resonance imaging breast density and reveals composition changes during neoadjuvant chemotherapy

Thomas D O'Sullivan[1], Anaïs Leproux[1], Jeon-Hor Chen[2,3], Shadfar Bahri[2], Alex Matlock[1], Darren Roblyer[1,*], Christine E McLaren[5,6], Wen-Pin Chen[5], Albert E Cerussi[1], Min-Ying Su[2], and Bruce J Tromberg[1*]

[1]Laser Microbeam and Medical Program, Beckman Laser Institute and Medical Clinic, University of California, 1002 Health Sciences Rd, Irvine, CA 92617, USA.

[2]Tu & Yuen Center for Functional Onco-Imaging, Department of Radiological Sciences, University of California, 164 Irvine Hall, Irvine, CA 92617, USA.

[3]Department of Radiology, E-Da Hospital and I-Shou University, 1 Yi-Da Road, Jiau-shu Tsuen, Yan-Chau Shiang, Kaohsiung 82445, Taiwan.

[4]Current address: Department of Biomedical Engineering, Boston University, 44 Cummington St, Boston, MA 02215, USA.

[5]Chao Family Comprehensive Cancer Center, University of California, Irvine Medical Center, 101 The City Drive, Orange, CA 92868, USA.

[6]Department of Epidemiology, University of California, 224 Irvine Hall, Irvine, CA, 92697 USA.

[*]Corresponding author: Bruce J Tromberg, bjtrombe@uci.edu

Abstract

Introduction: In addition to being a risk factor for breast cancer, breast density has been hypothesized to be a surrogate biomarker for predicting response to endocrine-based chemotherapies. The purpose of this study was to evaluate whether a non-invasive bedside scanner based on diffuse optical spectroscopic imaging (DOSI) provides quantitative metrics to measure and track changes in breast tissue composition and density. In order to access a broad range of densities in a limited patient population, we performed optical measurements on the contralateral normal breast of patients before and during neoadjuvant chemotherapy (NAC). In this work, DOSI parameters, including tissue hemoglobin, water, and lipid concentrations were obtained and correlated with magnetic resonance imaging (MRI)-measured fibroglandular tissue density. We evaluate how DOSI could be used to assess breast density while gaining new insight into the impact of chemotherapy on breast tissue.

Methods: This was a retrospective study of 28 volunteers undergoing NAC treatment for breast cancer. 3.0T MRI and broadband DOSI (650-1000nm) were obtained from the contralateral normal breast before and during NAC. Longitudinal DOSI measurements were used to calculate breast tissue concentrations of oxygenated and deoxygenated hemoglobin, water, and lipid. These values were compared to MRI-measured fibroglandular density before and during therapy.

Results: Water (r=0.843, p<0.001), deoxyhemoglobin (r=0.785, p=0.003), and lipid (r=-0.707, p=0.010) concentration measured by DOSI correlated strongly with MRI-measured density prior to therapy. Mean DOSI parameters differed significantly between pre- and post-menopausal subjects at baseline (water: p<0.001, deoxyhemoglobin: p=0.024, lipid: p=0.006). During NAC treatment measured at ~90 days, significant reductions were observed in oxyhemoglobin for pre- (-20.0%, 95% confidence interval (CI): -32.7 to -7.4) and post-

menopausal subjects (-20.1%, 95% CI: -31.4 to -8.8), and water concentration for pre-menopausal subjects (-11.9%, 95% CI: -17.1 to -6.7) compared to baseline. Lipid increased slightly in pre-menopausal subjects (3.8%, 95% CI: 1.1 to 6.5) and water increased slightly in post-menopausal subjects (4.4%, 95% CI: 0.1 to 8.6). Percent change in water at the end of therapy compared to baseline correlated strongly with percent change in MRI-measured density (r=0.864, p=0.012).

Conclusions: DOSI functional measurements correlate with MRI fibroglandular density, both prior to therapy and during NAC. Though a limited patient data set, these results suggest that DOSI may provide new functional indices of density based on hemoglobin and water that could be used at the bedside to assess response to therapy and evaluate disease risk.

Introduction

Breast density, an assessment of the volume fraction of the human breast which contains epithelial and connective tissues, is a risk factor for breast cancer. Numerous studies have shown that women presenting the highest density category evaluated from mammography have 4-6 fold increased cancer risk compared to women with lower density [1]. In addition, the International Breast Cancer Intervention Study (IBIS-I) primary chemoprevention study evaluating the selective estrogen receptor modulator (SERM) tamoxifen [2, 3] has revealed that only women who exhibited >10% reduction in percent mammographic density experienced tamoxifen's protective effect in decreased cancer incidence [4]. Women in the treated group who showed <10% decreased density had exactly the same cancer rates compared to the control group. Similar results were also recently found regarding the use of tamoxifen and aromatase inhibitors in the adjuvant setting [5]. These and related studies suggest that breast tissue density, in addition to being a risk factor, may also be a surrogate biomarker for monitoring, predicting, and optimizing individual response to hormonal therapies. However, methods to measure breast density by mammography or MRI have not been adopted for various reasons, preventing the utilization of breast density measurements in the clinic to assess risk or predict outcome.

To date, the only established criterion for assessing breast density is given by the Breast Imaging Reporting and Data System (BI-RADS) [6]. That system defines four categories for breast density, qualitatively based on the relative amounts of fat and dense fibroglandular tissue in a mammogram. While the system is useful for evaluating the probability that a tumor is obscured by dense tissue on a mammogram, it is not suitable for quantifying or measuring small changes in density. An alternative approach is to quantify PMD using computer-based image analysis techniques of mammograms [7-11]. While it is

possible to quantify density from the image, a 2D x-ray projection is inherently limited in its ability to accurately quantify longitudinal density changes [12]. The use of ionizing radiation also limits the frequency of measurements, making it unsuitable for monitoring adjuvant or preventative chemotherapy. We and others have investigated the use of MRI [12-19], which is a safe and quantitative technique for measuring breast density and volume, but its high cost precludes it from being applied for risk assessment and screening in most women.

Optical-based imaging modalities are a promising alternative to characterize breast density. Due to the absorption and scattering properties of breast tissue, near-infrared light (650-1,000 nm) is able to penetrate several centimeters deep. Researchers have measured breast tissue in transmission and reflectance geometries using continuous-wave spectroscopy, frequency-domain, or time-domain techniques [20, 21]. In order to correlate tissue optical measurements with breast density, several groups have compared spectroscopic features or measured tissue components (such as blood, water and lipid) with mammographic density. These optically-measured parameters have been compared against breast densities that have been qualitatively analyzed from mammograms, classified into only 3 or 4 density categories [22-28]. As mentioned earlier, this limits the ability of the measurement to detect small density changes. There has been promising work to correlate mammographic density with transillumination optical spectroscopy [29, 30], but these studies did not quantify tissue scattering and biochemical composition. This makes it difficult to compare patient spectroscopic features and link functional changes with underlying mechanisms of breast density.

We hypothesize that diffuse optical spectroscopic imaging (DOSI) provides quantitative metrics to measure and track changes in breast tissue composition and density. DOSI provides a quantitative measure of tissue functional components allowing for non-

invasive imaging of breast tissue composition and metabolism [31]. DOSI is capable of measuring tissue concentrations (ct) of oxygenated hemoglobin (ctO_2Hb), deoxygenated hemoglobin (ctHHb), water, and lipid. These measurements are directly related to tissue metabolism and vascular characteristics. For example, high levels of ctO_2Hb are considered to be a surrogate marker for elevated vascular supply and perfusion. High levels of ctHHb reflect high oxygen consumption and tissue metabolism due to cell proliferation and/or poor vascular drainage. Total hemoglobin (ctTHb) corresponds to the total blood volume in tissue and has been validated as an index that corresponds to increased vascular density [32].

DOSI scanning is performed without compression or injection of contrast agents using a bedside hand-held probe. Much of this work has been focused on determining functional changes in breast tumors during chemotherapy, a topic that is now under investigation in an American College of Radiology Imaging Networks (ACRIN) multi-center clinical trial [33]. The DOSI technique combines laser-based frequency-domain photon migration with broadband near-infrared spectroscopy to separate optical absorption and scattering over a broad spectral range [20]. This results in a quantitative data set of tissue concentrations that can be compared longitudinally in the same patient, or across different patients.

Our previous studies [34-36] have shown that pre-menopausal women tend to have greater water concentration than post-menopausal women, reflecting the high water content of epithelial connective-tissue compartments. Similarly pre-menopausal women have a higher hemoglobin concentration (both ctHHb and ctO_2Hb), due to greater vascular demands of the glandular tissue, and a lower lipid concentration. Based on this data we expect that breast density, which quantifies the abundance of hormonally-controlled glandular tissue, exhibits a positive correlation with water and ctTHb, and a negative correlation with lipid.

Since it is known that neoadjuvant chemotherapy (NAC) affects the density and

composition of normal breast [37], in this study we measured the contralateral normal side of breast cancer patients before and during NAC treatment with MRI and DOSI. We examined baseline composition, comparing differences between pre- and post-menopausal women. We analyzed DOSI parameters for markers of breast density and metabolism. The correlation between these results and fibroglandular tissue density measured by MRI was examined to test the hypothesis that DOSI can provide a quantitative measure of breast density. We further hypothesize that in addition to providing an optical index of breast density, DOSI may help provide insight into mechanisms of chemotherapy-induced changes in breast metabolism.

Methods

Subject measurements

This study is a retrospective analysis conducted on a subset of subjects with newly diagnosed, operative, primary breast cancer measured with DOSI or DOSI+MRI during their neoadjuvant chemotherapy treatment between 2007 and 2012. Subject demographics are shown in table 1. DOSI measurements were acquired at a minimum of 30 locations (taken in a rectangular grid pattern with 10mm spacing between measurement points) on a contralateral breast not suspicious for malignancies at two or more time points during the first 120 d of therapy (N=28). The DOSI+MRI cohort is a subset (N=12) of subjects who also received MRI imaging before NAC. Post-NAC MRI images were available for N=9 subjects.

All subjects provided informed written consent and participated in this study under clinical protocols approved by the Institutional Review Board at the University of California, Irvine (2002-2306, 2007-6084, and 2011-7812). Exclusion criteria included pregnant women and women who were less than 21 y old or more than 75 y old. All subjects were

histologically diagnosed with invasive carcinoma before neoadjuvant treatment.

DOSI measurement

A comprehensive description of the diffuse optical spectroscopic imaging (DOSI) system and underlying concepts are described elsewhere [38-40]. Briefly, the instrument combines frequency domain photon migration (FDPM) and continuous wave near-infrared spectroscopy (CW-NIRS) measurements to determine the optical scattering and absorption spectra (650–1,000 nm) of the measured tissue. The FDPM component consists of six laser diode sources (660, 680, 780, 810, 830, and 850 nm) that are sinusoidally intensity-modulated between 50 and 500 MHz. The relative amplitude and phase of the detected signals compared to the source are input into an analytical model of diffuse light transport to determine tissue scattering and absorption coefficients at these wavelengths. White light illumination at each measurement point is used for CW-NIRS spectroscopy. The detected broadband reflectance spectra are fit and scaled to the frequency domain scattering and absorption measurements in order to obtain full broadband absorption spectra over the entire spectral range. Absolute tissue concentrations are calculated by using the Beer–Lambert law and known extinction coefficient spectra of ctHHb, ctO_2Hb, water, and bulk lipid.

All subjects received NAC before surgical resection of tumors and were measured with the DOSI system before treatment (to establish a baseline measurement), and at several time points throughout their treatment. Based on our previous findings, baseline measurements were obtained at least 10 d after diagnostic biopsies to minimize their impact on DOSI scans [41]. Subjects were measured in a supine position. The DOSI probe was placed against the breast tissue, and sequential measurements were taken in a linear or rectangular grid pattern using 10-mm spacing. Measurement regions on the normal breast were taken to mirror the area of the underlying tumor determined by ultrasound and palpation

on the ipsilateral breast. Total measurement time varied between 20 min and 1 h per subject. Repeat DOSI scans have been shown previously to be relatively insensitive to probe contact pressure fluctuations, displaying less than 5% average variation in test–retest studies of human subjects [42].

Mammographic density analysis

Each subject was characterized by BI-RADS density category. In this system, category I is described as fatty breast tissue, II is scattered density, III is heterogeneously dense, and IV is extremely dense. The categories were compiled from pre-chemotherapy mammographic reports documented by the subjects' radiologists and were available for 20 of the 28 subjects. Of these, 4 subjects were BI-RADS density II, 11 subjects were BI-RADS III, and 5 subjects were BI-RADS IV.

MR imaging and breast density analysis

MR imaging examinations were performed by using a dedicated sensitivity-encoding–enabled bilateral four-channel breast coil with a 3.0 T system (Achieva; Philips Medical Systems, Best, the Netherlands) at timepoints before, during, and after completion of NAC. The axial view T1-weighted images without fat suppression were used for the analysis of breast density in this study. The images were acquired using a 2D turbo spin-echo pulse sequence with TR=800 ms, TE=8.6 ms, flip angle=90°, matrix size=480x480, FOV=31–38 cm, and slice thickness=2 mm.

The breast and fibroglandular tissue segmentation was performed using a modified published method [12, 43, 44]. Before the segmentation, the operator viewed the whole axial T1W images dataset and determined the superior and inferior boundaries of the breast (the beginning and ending slices) by comparing the thickness of breast fat with the body fat. The

breast segmentation procedures consisted of: 1) An initial horizontal line cut along the posterior margin of each individual subject's sternum to exclude thoracic region. 2) Applied Fuzzy-C-Means (FCM) clustering and b-spline curve fitting to obtain the breast-chest boundary. 3) A bias field correction method based on nonparametric nonuniformity normalization (N3) and adaptive FCM algorithm [44] was used to remove the strong intensity non-uniformity for segmentation of fibroglandular tissue and fatty tissue. 4) Applied dynamic searching to exclude the skin along the breast boundary. 5) The standard FCM algorithm was applied to classify all pixels on the image. The default setting is to use a total of 6 clusters, 3 for fibroglandular tissue and 3 for fatty tissues. After completing the segmentation processes in all image slices, the quantitative breast volume, fibroglandular tissue volume, and the percent density (calculated as the ratio of the fibroglandular tissue volume over the breast volume x100%), was calculated.

Neoadjuvant chemotherapy regimen

Most patients (N=19) received a 12-cycle, once a week course of a paclitaxel—either albumin-bound (nab-paclitaxel) or Cremophor-bound—and carboplatin. Other patients received only doxorubicin+cyclophosphamiden (AC therapy) (N=2), or received additional AC therapy either before (N=4) or after (N=2) paclitaxel+carboplatin. The remaining patient received docetaxel+carboplatin for 6 cycles, once every three weeks. Many patients also received bevacizumab as part of their treatment (N=15) and some HER2/neu positive patients also received trastuzumab (N=8).

Statistical analysis

Data description

Summary statistics including mean and standard error (SE) were calculated for the DOSI-

measured parameters of water, bulk lipid, ctO_2Hb, ctHHb, ctTHb, oxygen saturation (stO_2), and tumor optical index (TOI) measured at baseline and during NAC. TOI is a "tissue optical index" of metabolism that provides contrast for metabolically-active tissue, developed for identifying tumors [45], and is given by TOI = ctHHb × water / (% lipid). Subject measurements during NAC were recorded as having occurred in one of four intervals with interval midpoints 30 d (mean: 33.1; range 21-43 / N=16 pre-, N=11 post-menopausal), 60 d (mean: 60.8; range 55-69 / N=10 pre-, N=7 post-menopausal), 90 d (mean: 89.9; range 78-104 / N=16 pre-, N=9 post-menopausal), and 120 d (mean: 116.6; range 106-127 / N=6 pre-, N=4 post-menopausal) from the beginning of chemotherapy treatment.

Comparison of DOSI parameters between groups

The Mann-Whitney U test was applied to test whether mean values for DOSI parameters differed significantly between pre- and post-menopausal subjects. The Shapiro-Wilk test was applied to each DOSI parameter to test the fit to a normal distribution within BI-RADS categories II, III, and IV. Analysis of Variance (ANOVA) was applied to compare mean values among BI-RADS categories for water, lipid concentration, ctO_2Hb, ctHHb, ctTHb, and scattering power. The nonparametric Kruskal-Wallis test was applied to compare the distributions of stO_2 and TOI values among BI-RADS categories. For pairs of BI-RADS categories (II vs. III, II vs. IV, and III vs. IV), the mean values for DOSI parameters were compared with application of the Bonferroni-Holm method of adjustment for multiple comparisons to maintain an experiment-wise significance level of 0.05 for each DOSI parameter.

Regression and correlation analyses

The linear relationship between age and water concentration measured at baseline was assessed with linear regression analysis and Pearson's correlation coefficient. The influence

of values obtained from individual patients was assessed by examination of regression residuals and the DFFITS statistic. In addition, the correlation between age and change in water concentration at 90 d during NAC was estimated with Pearson's correlation coefficient.

The correlation between DOSI parameters and MRI fibroglandular density measured at baseline, as well as at 24 d and 82 d during NAC was assessed with Pearson's correlation coefficient. Similarly, the correlation between percent change in DOSI parameters and percent change in MRI fibroglandular density at 82 d of NAC (i.e. the end of NAC treatment) was assessed with Pearson's correlation coefficient. A significance level of 0.05 was used for assessment of estimated correlations.

Generalized estimating equations

We applied a statistical method known as generalized estimating equations (GEE) to estimate and compare the expected (mean) change from baseline for each specified DOSI parameter between pre- and post-menopausal subjects. For example, the GEE method was used to model the linear relationship between the mean change in breast tissue water as a function of predictors including menopausal status, measurement day after NAC, and the interaction between menopausal status and measurement day. Measurement day from the beginning of chemotherapy was represented by a categorical variable with four categories. In contrast to ordinary linear regression for which values measured in individual subjects are assumed to be independent, the GEE method takes in account the correlation between DOSI values measured within individual subjects. For application of the GEE, it is necessary to specify nature of the linear relationship between the mean value of the DOSI parameters and the predictors and between the mean and variance of DOSI parameter values. The nature of the within-subject correlations between DOSI measurements must also be specified. In technical language, we specified a normal model with an identity link function and an exchangeable

correlation structure. In brief, these specifications indicated that the mean and variance of DOSI parameter are related through a normal distribution and that the within-subject correlation between repeated measurements of DOSI values was assumed to be the same for each subject.

From the final GEE model for a given outcome, the estimated percent change from baseline was calculated and compared for both the pre- and post-menopausal groups 30, 60, 90, and 120 d from the beginning of chemotherapy. For analysis of each outcome, the Bonferroni-Holm method of adjustment for multiple comparisons was applied to maintain an experiment-wise significance level of 0.05.

Results

For each patient examination, tissue concentrations of ctO_2Hb, ctHHb, water, and lipid were calculated at each measurement point from the broadband absorption spectra. These data were used to construct 2D maps using a linear interpolation between measurement points, as shown in Figure 1. The areolar region provides significant contrast due to the high density of fibroglandular tissue and its increased metabolic activity. Optical absorption spectra of tissue in this region show higher concentrations of hemoglobin and reduced lipid content. For analysis, the average of DOSI measurement parameters (chromophore concentrations and scattering coefficients) was computed over the entire measurement region but excluding the areola. Since the areolar region is a concentrated region of fibroglandular tissue not representative of the breast as a whole, it was excluded from the DOSI average for this analysis; the nipple was also excluded from MRI segmentation of fibroglandular tissue. Identical measurement grids were used for longitudinal analysis.

Baseline pre- and post-menopausal differences

Figure 2 shows the average optical absorption and scattering spectra over all measurement points, excluding the areola, for all pre-menopausal (N=17) and post-menopausal (N=11) subjects. There are discernible differences in both the absorption and scattering spectra between pre-menopausal and post-menopausal women. Pre-menopausal women exhibit higher concentrations of hemoglobin, as evidenced by the overall higher absorption in the 670–850 nm range. There is also increased tissue water concentration relative to lipids in pre-menopausal women, as revealed by the large water absorption peak at 980 nm compared to the lipid peak at 930nm. Table 2 shows the absolute DOSI parameters for pre-menopausal, post-menopausal, and all subjects at baseline before beginning NAC treatment. In the absence of chemotherapeutic intervention, pre- and post-menopausal subjects exhibited statistically significant difference in means for water ($p<0.001$), lipid ($p=0.006$), ctHHb ($p=0.024$), and the tissue optical index (TOI) ($p=0.003$). Post-menopausal women had a lower mean ctHHb and mean water concentration at baseline than pre-menopausal women, and a higher mean lipid concentration. Figure 3 shows maps of TOI for a typical pre-menopausal and post-menopausal subject. In both subjects, the areolar region (indicated by the black line) exhibits much higher TOI than the surrounding tissue, while the surrounding TOI tends to be higher in the pre-menopausal subjects.

Because the mean tissue water concentration in the normal breast was significantly different at baseline between pre- and post-menopausal groups, the relationship between age and water concentration was examined to explore these differences in more detail. For a subgroup of N=27 subjects (one patient was excluded since she previously underwent an oophorectomy which caused premature menopause and confounds the effect of hormones on breast density), water concentration at baseline exhibited significant negative correlation (r=-

0.479, p=0.011) with age (Figure 4). One subject with extremely high breast density and corresponding water concentration (46.1%) exerted substantial influence on the regression coefficients as indicated by regression diagnostics. Previous studies by our group and others have shown that water concentration can vary dramatically in premenopausal patients [36, 46, 47], perhaps due to normal fluctuations caused by the menstrual cycle [48], which may account for the outlier.

Relationship between DOSI parameters and mammographic density categories

The relationships between DOSI parameters and mammographic density categories, based on the four traditional BI-RADS density categories, were assessed (Figure 5, all data shown in Additional file 1, Table S1.). None of the subjects measured were characterized as BI-RADS I. A statistically significant difference was found between BI-RADS density categories III and IV for ctO_2Hb, ctHHb, ctTHb, and TOI. Additionally a statistically significant difference was found between BI-RADS II and IV for water and TOI. Mean lipid concentration tended to decrease with increasing BI-RADS density category, and approached statistical significance. No significant difference in the means of stO_2 or scattering power was found.

Correlation between DOSI parameters and MRI breast density

The correlations between measured DOSI parameters and MRI fibroglandular tissue volume were examined at baseline and at various timepoints during NAC (table 3). At baseline, breast density calculated from MRI showed stronger correlations with ctHHb (r=0.785, p=0.003), water concentration (r=0.843, p<0.001), lipid (r=-0.707, p=0.010) and TOI (r=0.891, p<0.001) than with other measures. Figure 6 illustrates the linear relationship between water and ctHHb with breast density. A statistically significant correlation with ctTHb (r=0.597, p=0.040) was also demonstrated. Figure 7 displays the MR images and DOSI images at the beginning and end of NAC for a 31 year old pre-menopausal subject. This subject exhibited a

significant reduction in breast density during NAC, and similarly a significant reduction in water concentration. However, when correlations between MRI breast density and DOSI parameters were estimated at timepoints near the conclusion of NAC treatment (i.e. ~82 d), non-significant correlations were found ($p>0.05$ for all DOSI parameters). We also examined the correlation between percent change compared to baseline of the optical parameters and MRI fibroglandular density at ~82 d (table 4). There was a strong correlation of both *change* in water (r=0.864, p=0.012) and TOI (r=0.818, p=0.025) with MRI.

Variations in breast composition during NAC

Significant compositional changes of the normal breast were observed during NAC in both pre- and post-menopausal subjects with DOSI. GEE models that incorporated menopausal status and measurement day were used to fit the outcomes of percent change of DOSI parameter from baseline. Because most NAC regimens lasted 12 weeks, we show the GEE results at ~90 d from beginning of NAC treatment (Figure 8). The measured DOSI parameters at baseline before NAC and at ~30, 60, 90, and 120 d after the start of NAC are shown in Additional file 2, Table S1. Both the pre-menopausal (-20.0%, 95% CI: -32.7 to -7.4) and post-menopausal (-20.1%, 95% CI: -31.4 to -8.8) groups exhibited statistically significant decreases in ctO_2Hb while ctHHb stayed relatively flat (pre-menopausal: -2.5%, 95% CI: -7.7 to 2.7; post-menopausal: 0.5%, 95% CI: -5.3 to 6.3), yielding a reduction of ctTHb. Bulk lipids also remained relatively flat during NAC for both pre- (3.8%, 95% CI: 1.1 to 6.5) and post-menopausal (-0.4%, 95% CI: -3.4 to 2.6) groups. StO_2 was nearly identical between the two groups at baseline, and both decreased in a similar manner during NAC (pre-menopausal: -6.9%, 95% CI: -11.5 to -2.3; post-menopausal: -7.4%, 95% CI: -14.7 to 0.0). Scattering amplitude and power did not change appreciably during NAC, or between groups (data not shown).

Trends during NAC were similar in both menopause groups for all DOSI parameters except water (ctO_2Hb shown in Figure 9a), which exhibited a percent change that was statistically different between menopause groups at 90 d. Figure 9b shows that the pre-menopausal group incurred a steady decrease in tissue water during NAC, while breast tissue water concentration in the post-menopausal group remained flat. After 90 d of NAC, pre-menopausal subjects exhibited an estimated -11.9% (95% CI: -17.1,-6.7) reduction in breast tissue water concentration, while post-menopausal subjects showed an estimated increase of 4.4% (95% CI: 0.1 to 8.6). The percent change in water after 90 d of chemotherapy was correlated with age (Figure 9c, r=0.745, p<0.001), providing further evidence that effect of NAC on water concentration was stronger in younger, pre-menopausal subjects.

Discussion

Breast density is a strong independent risk factor for breast cancer and may also have a role in the risk of recurrence. Optical imaging is a low-cost imaging modality that shows promise for assessing breast density in the clinic without the use of ionizing radiation. Since optical imaging measures functional characteristics of tissue, it also yields additional information that complements breast density assessment techniques using MRI and mammography, which are primarily based on structure. This additional information may help to elucidate the origin of breast density and clarify causes of both natural and treatment-induced changes of breast density. By understanding the factors that modulate breast density and the source of its contrast in imaging, we will be able to better apply the parameter in risk assessment.

By and large, there is conflicting information in the literature correlating optically-measured tissue components with breast density. Most agree that increasing density correlates with increasing water concentration and ctTHb. However, there is conflicting data on other

measures, including bulk lipid that has found to be negatively correlated with density [27], or not at all [24]. Oxygen saturation (the fraction of ctO_2Hb to ctTHb, or StO_2) has been shown to be reduced in dense tissue [25], while others do not find a significant correlation [24, 27]. In addition, Taroni et al has included collagen as a basis chromophore and found that it is strongly associated with BI-RADS categories II-IV [27]. Optical scattering is also expected to increase with greater breast density due to the underlying fibroglandular structures, and some studies have indeed shown this [25, 27]. It is possible that these disagreements are due to the broad classification of density categories, the limited ability of the applied optical modalities to accurately quantify tissue components, or some combination of the two.

In this study, we found that water, ctO_2Hb, ctHHb, ctTHb, and TOI are associated with BI-RADS density category, while lipid tended to decrease with increasing category but was not statistically significant. The largest mean differences in hemoglobin were found between BI-RADS density categories III and IV, but not category II and IV. This contradiction is likely due to the small sample size (N=4 with BI-RADS II) and the limitations of a broad density classification scheme. We expect lipid to be significantly associated with BI-RADS category in a larger sample size. There was no association discovered between stO_2 or scattering power with BI-RADS density.

Several DOSI parameters were strongly correlated with MRI fibroglandular breast density measured at baseline, including tissue water, lipid, and ctHHb concentrations. There was no significant correlation between density and scattering parameters or StO_2. This significant correlation with water is likely due to the fact that fibroglandular tissue has ~30% higher water content than adipose tissue [24]. These observations are in general agreement with the findings of other groups, with the addition that here we have shown, for the first time, that a quantitative measure of water can be compared longitudinally and between

patients. Because DOSI is a measurement of chromophore concentration throughout the probed tissue volume, the increased water may also be due to the increased vascular supply required by the dense tissue. Furthermore, we demonstrated a strong baseline correlation between ctHHb and breast density, reflecting the increased rate of metabolism in fibroglandular breast tissue. Because metabolism is strongly captured in the tissue optical index (TOI), this metric was also shown to be a good predictor of breast density. Finally, greater hemoglobin concentrations were observed in patients with dense breasts suggesting greater vascular density in these subjects, and lower lipid concentrations as would be expected by replacement of fibroglandular tissue with adipose.

At baseline, we observed statistically significant differences in the breast composition and indicators of metabolism for pre-menopausal and post-menopausal groups, confirming previous studies [47]. There were increased mean ctHHb and mean water concentrations as well as decreased mean bulk lipid concentration in the breast of pre-menopausal subjects, compared to those of post-menopausal subjects. This is all consistent with increased cell proliferation and metabolic activity in the denser breast tissue of younger pre-menopausal women.

Significant changes in optical markers for vascular density and supply (ctO_2Hb and water) were observed during NAC treatment. A significant decrease in ctO_2Hb was observed in both pre-menopausal and post-menopausal groups. The steady reduction of ctO_2Hb without a corresponding decrease in ctHHb suggests that NAC agents act directly on the breast tissue perhaps by causing a reduction of perfusion. This may be caused by chemotherapy-induced vascular damage and may contribute to the reduction of breast density. In contrast, only pre-menopausal subjects experienced a significant loss of water in their breast tissue during NAC. This trend better matches the observed effect of NAC on

MRI-measured breast density wherein premenopausal subjects experience a greater loss [37]. Even though the absolute DOSI parameters were not significantly correlated with MRI measurements at the end of NAC, the percent change in water and TOI at the end of treatment compared to baseline did show strong correlation with the percent change in fibroglandular breast density over the same time.

These NAC-induced changes could potentially have been caused by direct anti-proliferative effects of chemotherapy, or by the indirect effect of ovarian suppression and subsequent hormone level reductions [37]. Cytoxic chemotherapeutic agents are known to cause suppression of ovarian function and amenorrhea while ovarian-secreted hormones (estrogen and progesterone) are known to increase breast density [49-51]. The greater reduction in breast tissue water in younger, pre-menopausal subjects suggests that their chemo-reduced ovarian hormone levels may have a role in reducing breast tissue density. Consequently, the change in ctO_2Hb also suggests a mechanism that is hormone-independent. The enhanced breast density reduction in pre-menopausal subjects could also be due to the fact that breast tissue naturally becomes less dense with age [52, 53]. Evidence suggests that this is also a hormonal effect [49-51]; however it is due to natural aging and not induced by the chemotherapy. This is reflected in the reduced baseline water concentration of older subjects. If there is less fibroglandular tissue present in the breast of the older women, then it is possible that NAC may not be able to cause a significant change in breast density (i.e. it has already been reduced to minimum). This complicates the ability to separate the relative importance of chemotherapy as a direct or indirect modulator of breast density.

We note that relatively little change over time was observed in mean DOSI-measured bulk lipid in both groups of patients undergoing NAC. This suggests that the rapid changes in breast density induced by NAC occur due to the reduction of the fibroglandular tissue rather

than by increases or replacement by bulk lipid.

This study is limited because it is a retrospective study and includes a small number of subjects, especially those with matched DOSI and MRI measurements. Therefore, the reported correlations should be interpreted with caution, and they point to the need for further studies. Furthermore, DOSI measurements did not sample the entire breast volume. Recent data have shown, however, that density-related measurements from a spatially-limited optical sampling on the breast are strongly associated with BI-RADS category [28]. Multiple therapy regimens were included in the analysis, and it is likely the underlying changes in breast density vary based on the specific chemotherapy drugs given. Future work stratifying DOSI changes by treatment type and outcome in a larger population may provide insight into mechanisms of these changes as well as patient response to therapy. Additionally, timing of the subjects' menstrual cycles were not accounted for, which can cause variations in breast density, as well as their pregnancy history. Nonetheless, the ability to identify significant correlations over several years of optical measurements speaks to the strength of the DOSI method as a promising quantitative tool.

Conclusions

In conclusion, this is the first study to confirm that optical imaging can detect significant compositional and functional changes in the contralateral normal breast before and during chemotherapy, and these changes are correlated with MRI anatomic measurements of breast density. Density is a strong independent risk factor for breast cancer, and the ability to quantify it could be valuable input to breast cancer risk models. Imaging biomarkers could be used to provide individualized treatment and predict response as well as risk of recurrence in breast cancer patients. Together with tissue analysis, DOSI may provide insight into the

underlying biological origin of density and improve our understanding of the chemo- and hormonal therapy effects. Prospective studies need to be performed to further understand the correlation of parameters measured by DOSI and MRI breast imaging modalities. If validated, DOSI may provide an alternative approach to predict cancer risk as well as monitor the protective effects of cancer therapies.

Abbreviations

AC – doxorubicin+cyclophosphamide chemotherapy regimen; ACRIN – American College of Radiology Imaging Network; ANOVA—analysis of variance; BI-RADS – Breast Imaging-Reporting and Data System; CI – confidence interval; ct – concentration; ctHHb – tissue concentration of deoxyhemoglobin; ctO_2Hb – tissue concentration of oxyhemoglobin; ctTHb – tissue concentration of total hemoglobin; CW-NIRS – continuous-wave near-infrared spectroscopy; DFFITS – diagnostic to assess the influence of a single point in a statistical regression; DOSI – diffuse optical spectroscopic imaging; FCM – fuzzy-C-Means; FDPM – frequency-domain photon migration; FOV – field of view; GEE – generalized estimating equations; HER2 – human epidermal growth factor receptor 2; IBIS-I – International Breast Cancer Intervention Study – I; MRI – magnetic resonance imaging; NAC – neoadjuvant chemotherapy; SE – standard error; SERM – selective estrogen receptor modulator; stO_2 – tissue oxygen saturation; TE – echo time (in MR imaging); TOI – tissue optical index; TR – repetition time (in MR imaging).

Competing interests

A. Cerussi and B.J. Tromberg report patents, which are owned by the University of

California, that are related to the technology and analysis methods described in this study. The Institutional Review Board and Conflict of Interest Office of the University of California, Irvine, have reviewed both patent and corporate disclosures and did not find any concerns. No potential conflicts of interest were disclosed by the other authors.

Acknowledgements

The authors wish to thank Montana Compton and Amanda F. Durkin for their assistance as well as the patients who generously volunteered for this study. This work was supported by National Institutes of Health Grants P41RR01192 and P41EB015890 (Laser Microbeam and Medical Program), U54-CA105480 (Network for Translational Research in Optical Imaging), U54-CA136400, R01-CA142989, R01-CA127927, NCI-2P30CA62203 (University of California, Irvine Cancer Center Support Grant), Air Force Research Laboratory Agreement Number FA9550-04-1-0101, and NCI-T32CA009054 (University of California, Irvine Institutional Training Grant). Beckman Laser Institute programmatic support from the Arnold and Mabel Beckman Foundation is gratefully acknowledged.

Author contributions

TO designed the study, carried out the data processing and analysis, and drafted the manuscript. AL, JC, SB, DR, and AC assisted with data collection, processing and analysis. AM assisted with data processing while CM and WC performed statistical analyses and assisted with interpretation of results. MS and BJT conceived of the study, participated in its design and coordination and helped to draft the manuscript. All authors read and approved the final manuscript.

References

1. Boyd NF, Dite GS, Stone J, Gunasekara A, English DR, McCredie MRE, Giles GG, Tritchler D, Chiarelli A, Yaffe MJ, Hopper JL: **Heritability of mammographic density, a risk factor for breast cancer.** *New Engl J Med* 2002, **347:**886-894.

2. Cuzick J, Forbes J, Edwards R, Baum M, Cawthorn S, Coates A, Hamed H, Howell A, Powles T, Clunie G, Collins R, Day N, Northover J, IBIS Investigators: **First results from the International Breast Cancer Intervention Study (IBIS-1): a randomised prevention trial.** *Lancet* 2002, **360:**817-824.

3. Cuzick J, Forbes JF, Sestak I, Cawthorn S, Hamed H, Holli K, Howell A: **Long-Term Results of Tamoxifen Prophylaxis for Breast Cancer—96-Month Follow-up of the Randomized IBIS-I Trial.** *Journal of the National Cancer Institute* 2007, **99:**272-282.

4. Cuzick J, Warwick J, Pinney E, Duffy SW, Cawthorn S, Howell A, Forbes JF, Warren RML: **Tamoxifen-induced reduction in mammographic density and breast cancer risk reduction: a nested case–control study.** *J Natl Cancer I* 2011, **103:**744-752.

5. Kim J, Han W, Moon H-G, Ahn S, Shin H-C, You J-M, Han S-W, Im S-A, Kim T-Y, Koo H, Chang J, Cho N, Moon W, Noh D-Y: **Breast density change as a predictive surrogate for response to adjuvant endocrine therapy in hormone receptor positive breast cancer.** *Breast Cancer Res* 2012, **14:**R102.

6. *BI-RADS Breast Imaging Reporting and Data System Breast Imaging Atlas.* Reston, VA: American College of Radiology; 2003.

7. Byng JW, Boyd NF, Fishell E, Jong RA, Yaffe MJ: **The quantitative analysis of mammographic densities.** *Phys Med Biol* 1994, **39:**1629.

8. Glide-Hurst CK, Duric N, Littrup P: **A new method for quantitative analysis of mammographic density.** *Med Phys* 2007, **34:**4491-4498.

9. Harvey JA, Bovbjerg VE: **Quantitative Assessment of Mammographic Breast Density: Relationship with Breast Cancer Risk1.** *Radiology* 2004, **230:**29-41.

10. Martin KE, Helvie MA, Zhou C, Roubidoux MA, Bailey JE, Paramagul C, Blane CE, Klein KA, Sonnad SS, Chan H-P: **Mammographic Density Measured with Quantitative Computer-aided Method: Comparison with Radiologists' Estimates and BI-RADS Categories.** *Radiology* 2006, **240:**656-665.

11. Zhou C, Chan H-P, Petrick N, Helvie MA, Goodsitt MM, Sahiner B, Hadjiiski LM: **Computerized image analysis: Estimation of breast density on mammograms.** *Med Phys* 2001, **28:**1056-1069.

12. Nie K, Chen J-H, Chan S, Chau M-K, Yu HJ, Bahri S, Tseng T, Nalcioglu O, Su M-Y: **Development of a quantitative method for analysis of breast density based on three-dimensional breast MRI.** *Med Phys* 2008, **35:**5253-5262.

13. Graham SJ, Bronskill MJ, Byng JW, Yaffe MJ, Boyd NF: **Quantitative correlation of breast tissue parameters using magnetic resonance and X-ray mammography.** *Br J Cancer* 1996, **73:**162-168.

14. Lee NA, Rusinek H, Weinreb J, Chandra R, Toth H, Singer C, Newstead G: **Fatty and fibroglandular tissue volumes in the breasts of women 20-83 years old: comparison of X-ray mammography and computer-assisted MR imaging.** *AJR*

Am J Roentgenol 1997, **168:**501-506.

15. Li L, Chu Y, Salem AF, Clark RA: **Image segmentation and 3D visualization for MRI mammography.** In *SPIE Medical Imaging 2002: Image Processing; San Diego, CA, USA*. Edited by Sonka M, Fitzpatrick JM. 2002: 1780-1789.

16. Klifa C, Carballido-Gamio J, Wilmes L, Laprie A, Lobo C, DeMicco E, Watkins M, Shepherd J, Gibbs J, Hylton N: **Quantification of breast tissue index from MR data using fuzzy clustering.** In *Engineering in Medicine and Biology Society, 2004 IEMBS '04 26th Annual International Conference of the IEEE*; *1-5 Sept. 2004*. 2004: 1667-1670.

17. Wei J, Chan H-P, Helvie MA, Roubidoux MA, Sahiner B, Hadjiiski LM, Zhou C, Paquerault S, Chenevert T, Goodsitt MM: **Correlation between mammographic density and volumetric fibroglandular tissue estimated on breast MR images.** *Med Phys* 2004, **31:**933-942.

18. Yao J, Zujewski JA, Orzano J, Prindiville S, Chow C: **Classification and calculation of breast fibroglandular tissue volume on SPGR fat suppressed MRI.** In *SPIE Medical Imaging 2005: Image Processing; San Diego, CA, USA*. Edited by Fitzpatrick JM, Reinhardt JM. SPIE; 2005: 1942-1949.

19. van Engeland S, Snoeren PR, Huisman H, Boetes C, Karssemeijer N: **Volumetric breast density estimation from full-field digital mammograms.** *IEEE T Med Imaging* 2006, **25:**273-282.

20. O'Sullivan TD, Cerussi AE, Cuccia DJ, Tromberg BJ: **Diffuse optical imaging using spatially and temporally modulated light.** *J Biomed Opt* 2012, **17:**071311-071314.

21. Taroni P: **Diffuse optical imaging and spectroscopy of the breast: A brief outline of history and perspectives.** *Photochem Photobiol* 2012.

22. Blackmore KM, Knight JA, Jong R, Lilge L: **Assessing breast tissue density by transillumination breast spectroscopy (TIBS): an intermediate indicator of cancer risk.** *Br J Radiol* 2007, **80:**545-556.

23. Blyschak K, Simick M, Jong R, Lilge L: **Classification of breast tissue density by optical transillumination spectroscopy: Optical and physiological effects governing predictive value.** *Med Phys* 2004, **31:**1398-1414.

24. Brooksby B, Pogue BW, Jiang S, Dehghani H, Srinivasan S, Kogel C, Tosteson TD, Weaver J, Poplack SP, Paulsen KD: **Imaging breast adipose and fibroglandular tissue molecular signatures by using hybrid MRI-guided near-infrared spectral tomography.** *Proc Natl Acad Sci U S A* 2006, **103:**8828-8833.

25. Srinivasan S, Pogue BW, Carpenter C, Jiang S, Wells WA, Poplack SP, Kaufman PA, Paulsen KD: **Developments in Quantitative Oxygen-Saturation Imaging of Breast Tissue In Vivo Using Multispectral Near-Infrared Tomography.** *Antioxid Redox Sign* 2007, **9:**1143-1156.

26. Srinivasan S, Pogue BW, Jiang S, Dehghani H, Kogel C, Soho S, Gibson JJ, Tosteson TD, Poplack SP, Paulsen KD: **In Vivo Hemoglobin and Water Concentrations, Oxygen Saturation, and Scattering Estimates From Near-Infrared Breast Tomography Using Spectral Reconstruction.** *Acad Radiol* 2006, **13:**195-202.

27. Taroni P, Pifferi A, Quarto G, Spinelli L, Torricelli A, Abbate F, Villa A, Balestreri N, Menna S, Cassano E, Cubeddu R: **Noninvasive assessment of breast cancer risk using time-resolved diffuse optical spectroscopy.** *J Biomed Opt* 2010, **15:**060501.

28. Taroni P, Pifferi A, Quarto G, Spinelli L, Torricelli A, Abbate F, Balestreri N, Ganino S, Menna S, Cassano E, Cubeddu R: **Effects of tissue heterogeneity on the optical estimate of breast density.** *Biomed Opt Express* 2012, **3:**2411-2418.

29. Blackmore KM, Dick S, Knight J, Lilge L: **Estimation of mammographic density on an interval scale by transillumination breast spectroscopy.** *J Biomed Opt* 2008, **13:**064030.

30. Blackmore KM, Knight JA, Lilge L: **Association between transillumination breast spectroscopy and quantitative mammographic features of the breast.** *Cancer Epidem Biomar* 2008, **17:**1043-1050.

31. Cerussi A, Hsiang D, Shah N, Mehta R, Durkin A, Butler J, Tromberg BJ: **Predicting response to breast cancer neoadjuvant chemotherapy using diffuse optical spectroscopy.** *Proc Natl Acad Sci U S A* 2007, **104:**4014-4019.

32. Pakalniskis MG, Wells WA, Schwab MC, Froehlich HM, Jiang S, Li Z, Tosteson TD, Poplack SP, Kaufman PA, Pogue BW, Paulsen KD: **Tumor Angiogenesis Change Estimated by Using Diffuse Optical Spectroscopic Tomography: Demonstrated Correlation in Women Undergoing Neoadjuvant Chemotherapy for Invasive Breast Cancer?** *Radiology* 2011, **259:**365-374.

33. **Monitoring and Predicting Breast Cancer Neoadjuvant Chemotherapy Response Using Diffuse Optical Spectroscopic Imaging (DOSI)** [http://www.acrin.org/TabID/681/Default.aspx]

34. Shah N, Cerussi A, Eker C, Espinoza J, Butler J, Fishkin J, Hornung R, Tromberg B: **Noninvasive functional optical spectroscopy of human breast tissue.** *Proceedings of the National Academy of Sciences* 2001, **98:**4420-4425.

35. Tromberg BJ, Shah N, Lanning R, Cerussi A, Espinoza J, Pham T, Svaasand L, Butler J: **Non-invasive in vivo characterization of breast tumors using photon migration spectroscopy.** *Neoplasia* 2000, **2:**26-40.

36. Cerussi AE, Berger AJ, Bevilacqua F, Shah N, Jakubowski D, Butler J, Holcombe RF, Tromberg BJ: **Sources of Absorption and Scattering Contrast for Near-Infrared Optical Mammography.** *Acad Radiol* 2001, **8:**211-218.

37. Chen J-H, Nie K, Bahri S, Hsu C-C, Hsu F-T, Shih H-N, Lin M, Nalcioglu O, Su M-Y: **Decrease in Breast Density in the Contralateral Normal Breast of Patients Receiving Neoadjuvant Chemotherapy: MR Imaging Evaluation 1.** *Radiology* 2010, **255:**44-52.

38. Bevilacqua F, Berger AJ, Cerussi AE, Jakubowski D, Tromberg BJ: **Broadband Absorption Spectroscopy in Turbid Media by Combined Frequency-Domain and Steady-State Methods.** *Appl Opt* 2000, **39:**6498-6507.

39. Jakubowski D, Bevilacqua F, Merritt S, Cerussi A, Tromberg BJ: **Quantitative Absorption and Scattering Spectra in Thick Tissues Using Broadband Diffuse Optical Spectroscopy.** In *Biomedical Optical Imaging.* Edited by Fujimoto JG, Farkas DL: Oxford University Press; 2009: 330-355

40. Pham TH, Coquoz O, Fishkin JB, Anderson E, Tromberg BJ: **Broad bandwidth frequency domain instrument for quantitative tissue optical spectroscopy.** *Rev Sci Instrum* 2000, **71:**2500-2513.

41. Tanamai W, Chen C, Siavoshi S, Cerussi A, Hsiang D, Butler J, Tromberg B: **Diffuse optical spectroscopy measurements of healing in breast tissue after core biopsy: case study.** *J Biomed Opt* 2009, **14:**014024-014029.

42. Cerussi A, Siavoshi S, Durkin A, Chen C, Tanamai W, Hsiang D, Tromberg BJ: **Effect of contact force on breast tissue optical property measurements using a broadband diffuse optical spectroscopy handheld probe.** *Appl Opt* 2009, **48:**4270-4277.

43. Chang DHE, Chen J-H, Lin M, Bahri S, Yu HJ, Mehta RS, Nie K, Hsiang DJB, Nalcioglu O, Su M-Y: **Comparison of breast density measured on MR images acquired using fat-suppressed versus nonfat-suppressed sequences.** *Med Phys* 2011, **38:**5961-5968.

44. Lin M, Chan S, Chen J-H, Chang D, Nie K, Chen S-T, Lin C-J, Shih T-C, Nalcioglu O, Su M-Y: **A new bias field correction method combining N3 and FCM for improved segmentation of breast density on MRI.** *Med Phys* 2011, **38:**5-14.

45. Tromberg B, Cerussi A, Shah N, Compton M, Durkin A, Hsiang D, Butler J, Mehta R: **Imaging in breast cancer: Diffuse optics in breast cancer: detecting tumors in pre-menopausal women and monitoring neoadjuvant chemotherapy.** *Breast Cancer Res* 2005, **7:**279-285.

46. Cubeddu R, D'Andrea C, Pifferi A, Taroni P, Torricelli A, Valentini G: **Effects of the Menstrual Cycle on the Red and Near-infrared Optical Properties of the Human Breast.** *Photochem Photobiol* 2000, **72:**383-391.

47. Shah N, Cerussi AE, Jakubowski D, Hsiang D, Butler J, Tromberg BJ: **Spatial variations in optical and physiological properties of healthy breast tissue.** *J Biomed Opt* 2004, **9:**534-540.

48. Pogue BW, Jiang S, Dehghani H, Kogel C, Soho S, Srinivasan S, Song X, Tosteson TD, Poplack SP, Paulsen KD: **Characterization of hemoglobin, water, and NIR**

scattering in breast tissue: analysis of intersubject variability and menstrual cycle changes. *J Biomed Opt* 2004, **9:**541-552.

49. Bremnes Y, Ursin G, Bjurstam N, Rinaldi S, Kaaks R, Gram IT: **Endogenous sex hormones, prolactin and mammographic density in postmenopausal Norwegian women.** *Int J Cancer* 2007, **121:**2506-2511.

50. Noh JJ, Maskarinec G, Pagano I, Cheung LWK, Stanczyk FZ: **Mammographic densities and circulating hormones: A cross-sectional study in premenopausal women.** *The Breast* 2006, **15:**20-28.

51. Ursin G, Astrahan MA, Salane M, Parisky YR, Pearce JG, Daniels JR, Pike MC, Spicer DV: **The detection of changes in mammographic densities.** *Cancer Epidemiol Biomarkers Prev* 1998, **7:**43-47.

52. Clemons M, Goss P: **Estrogen and the Risk of Breast Cancer.** *New Engl J Med* 2001, **344:**276-285.

53. Kelemen LE, Pankratz VS, Sellers TA, Brandt KR, Wang A, Janney C, Fredericksen ZS, Cerhan JR, Vachon CM: **Age-specific Trends in Mammographic Density.** *Am J Epidemiol* 2008, **167:**1027-1036.

Figure 1. Diffuse optical spectroscopic imaging (DOSI) measurement schematic. A two-dimensional map of functional properties is generated by measuring broadband absorption and scattering spectra in a grid pattern. On the left is a grid (10 mm) where each dot represents a DOSI measurement point. The middle shows a map of lipid concentration (actual breast data) generated from the measured spectra on the right. Note that the areola region (A)

has much less lipid concentration and overall higher optical absorption compared to the rest of the breast (B) due to the higher concentration of water and hemoglobin in fibroglandular tissue.

Figure 2. Average absorption and scattering spectra measured at baseline for pre-menopausal (N=17) and post-menopausal (N=11) subjects. First, the average value was computed for measurements within each subject, and then the means for the resulting spectra over all subjects were computed. Error bars represent standard error.

Figure 3. Typical maps of tissue optical index (TOI) in the breast of a pre-menopausal and post-menopausal subject at baseline. The outer limit of the areolar region is indicated by the black line. Tick mark separation equals 1 cm. ctHHb, deoxyhemoglobin concentration

Figure 4. Breast tissue water concentration at baseline decreased with age (*r*=-0.479, p=0.011). Data shown is for N=27 pre- and post-menopausal subjects (one patient was excluded since she previously underwent an oophorectomy, confounding the effect of hormones on breast density).

Figure 5. The mean value of measured diffuse optical spectroscopic imaging parameters, separated by the Breast Imaging-Reporting and Data System (BI-RADS) density category. A statistically significant difference (noted with an asterisk) was found between BI-RADS density categories III and IV for oxyhemoglobin (ctO_2Hb), deoxyhemoglobin (ctHHb), total hemoglobin (ctTHb), and tissue optical index (TOI). Additionally a statistically significant difference was found between BI-RADS II and IV for water and TOI. Error bars represent standard error.

Figure 6. Correlation between optically-measured deoxyhemoglobin (ctHHb) and water with fibroglandular density measured by magnetic resonance imaging (MRI). Data is

for N=12 subjects (all subjects in which we had available corresponding data) at baseline before chemotherapy (N=9 pre- and N=3 post-menopausal). The fitted linear regression line is superimposed on the graph.

Figure 7. Corresponding magnetic resonance imaging (MRI) and diffuse optical spectroscopic imaging (DOSI). Images were taken at baseline and end of neoadjuvant chemotherapy in the contralateral normal breast of a pre-menopausal patient. The yellow outlines in the MRI images depict the result of the segmentation algorithm for fibroglandular tissue in the shown slices. The DOSI maps depict measured parameters as a function of position (tick mark separation equals 1 cm). The illustrated maps are from an 8 x 6 cm area from the upper-inner region of the left breast. The areolar region has more water, outlined by the semi-circle. The decreased density after chemotherapy is clearly visible in both MRI and DOSI. MRI shows 30.4% reduction in fibroglandular tissue volume and DOSI shows 24.4% reduction in tissue water. ctHHb, deoxyhemoglobin concentration; TOI, tissue optical index

Figure 8. Percent change in water, deoxyhemoglobin (ctHHb), oxyhemoglobin (ctO_2Hb), Lipid, and tissue oxygen saturation (StO_2) at 90 d of chemotherapy treatment compared with baseline. Based on longitudinal generalized estimating equation models, a statistically significant difference in water (noted with an asterisk) was found between pre-menopausal and post-menopausal groups. Error bars represent standard error.

Figure 9. Optically-measured changes over time during chemotherapy. a) Oxyhemoglobin decreased during chemotherapy (90 d) for both groups of patients; b) Water concentration decreased in pre-menopausal patients during chemotherapy, and remained relatively unchanged in post-menopausal patients. c) The reduction of water observed after 90 d of chemotherapy was associated with age (r=0.745, $p<0.001$), with younger subjects exhibiting a greater reduction. Data shown is for N=24 pre- and post-menopausal subjects in

which we had measurement data at 90 d (one patient was excluded since she previously underwent an oophorectomy, confounding the effect of hormones on breast density). The fitted linear regression line is superimposed on the graph.

Table 1. Subject demographics. DOSI, diffuse optical spectroscopic imaging; MRI, magnetic resonance imaging.

	Age (years) Mean ± SD	Number
DOSI cohort	47.4 ± 10.2	28
- Pre-menopausal	40.8 ± 5.0	17
- Post-menopausal	57.6 ± 7.2	11
DOSI+MRI cohort	43.6 ± 11.0	12
- Pre-menopausal	38.l ± 5.3	9
- Post-menopausal	60.0 ± 4.0	3

Table 2. Absolute tissue concentrations (mean ± standard error) measured in the normal breast at baseline.

	Water (%)	Lipid (%)	ctO2Hb (µM)	ctHHb (µM)	ctTHb (µM)	stO_2 (%)	TOI
All n=28	21.4 ± 1.3	69.7 ± 1.3	18.0 ± 1.2	5.0 ± 0.2	23.0 ± 1.3	77.2 ± 0.9	1.7 ± 0.2
Pre n=17	24.4 ± 1.8***	67.0 ± 1.6**	18.9 ± 1.7	5.3 ± 0.2*	24.2 ± 1.9	76.8 ± 1.1	2.1 ± 0.3**
Post n=11	16.6 ± 0.7***	74.0 ± 1.4**	16.6 ± 1.5	4.5 ± 0.2*	21.1 ± 1.6	77.7 ± 1.7	1.0 ± 0.1**

Data are shown for all patients, and for the pre-menopausal (pre) and post-menopausal (post) subgroups. ctO_2Hb, oxyhemoglobin concentration; ctHHb, deoxyhemoglobin concentration; ctTHb, total hemoglobin concentration; stO_2, tissue oxygen saturation; TOI, tissue optical index. *, ** denote a statistically significant difference (Mann-Whitney U test) between pre- and post-menopausal groups ($p<0.05$, $p<0.01$, $p<0.001$ respectively).

Table 3. Correlation between diffuse optical spectroscopic imaging parameters and fibroglandular density measured by magnetic resonance imaging for subjects at baseline and timepoints during chemotherapy.

	Baseline (N=12)		~25 d (N=10) Mean: 24.8 ± 5.5		~82 d (N=7) Mean: 82.4 ± 11.9	
	R	p	*r*	p	*r*	P
Water	**0.843**	**<0.001**	**0.675**	**0.032**	0.405	0.367
Lipid	**-0.707**	**0.010**	-0.462	0.179	-0.018	0.970
ctO_2Hb	0.557	0.060	**0.647**	**0.043**	0.464	0.294
ctHHb	**0.785**	**0.003**	0.399	0.253	0.705	0.077
ctTHb	**0.597**	**0.040**	**0.644**	**0.045**	0.599	0.155
stO_2	0.196	0.543	0.240	0.505	0.012	0.979
TOI	**0.891**	**<0.001**	0.541	0.107	0.593	0.160
Scat. Power	0.205	0.523	0.143	0.694	0.265	0.566

Bold values indicate statistical significance at the 0.05 level. ctO_2Hb, oxyhemoglobin concentration; ctHHb, deoxyhemoglobin concentration; ctTHb, total hemoglobin concentration; stO_2, tissue oxygen saturation; TOI, tissue optical index

Table 4. Correlation between percent change in optical parameters and percent change in fibroglandular density by magnetic resonance imaging.

	r	p
Water	**0.864**	**0.012**
Lipid	-0.502	0.251
ctO_2Hb	-0.166	0.721
ctHHb	0.606	0.149
ctTHb	0.017	0.971
stO_2	-0.412	0.357
TOI	**0.818**	**0.025**
Scat. Power	0.195	0.675

Data is for the N=7 subjects measured at ~82 d of chemotherapy (N=5 pre- and N=2 post-menopausal). Bold values indicate statistical significance at the 0.05 significance level. ctO_2Hb, oxyhemoglobin concentration; ctHHb, deoxyhemoglobin concentration; ctTHb, total hemoglobin concentration; stO_2, tissue oxygen saturation; TOI, tissue optical index.

Additional files

Additional file 1

Title: Comparison of diffuse optical spectroscopic imaging parameters by density category.

Description: This table provides the mean and standard error in each diffuse optical spectroscopic imaging parameter for the pairwise comparison of Breast Imaging Reporting and Data System (BI-RADS) density classifications.

Additional file 2

Title: Chromophore concentrations in the contralateral normal breast measured at baseline and during neoadjuvant chemotherapy.

Description: This table provides the absolute chromophore concentrations measured by diffuse optical spectroscopic imaging (DOSI) in the normal breast at baseline and at timepoints during neoadjuvant chemotherapy.

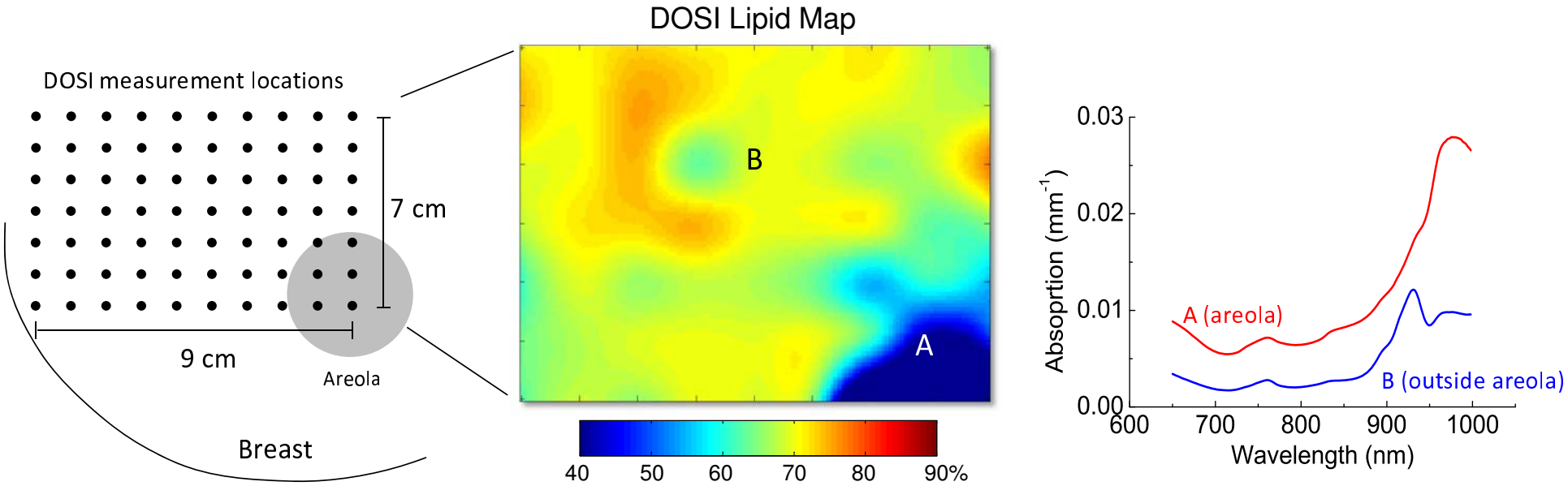
DOSI measurement locations
7 cm
9 cm
Areola
Breast
DOSI Lipid Map
B
A
40
50
60
70
80
90%
Absoprtion (mm-1)
0.03
0.02
0.01
0.00
A (areola)
B (outside areola)
600
700
800
900
1000
Wavelength (nm)

Figure 1

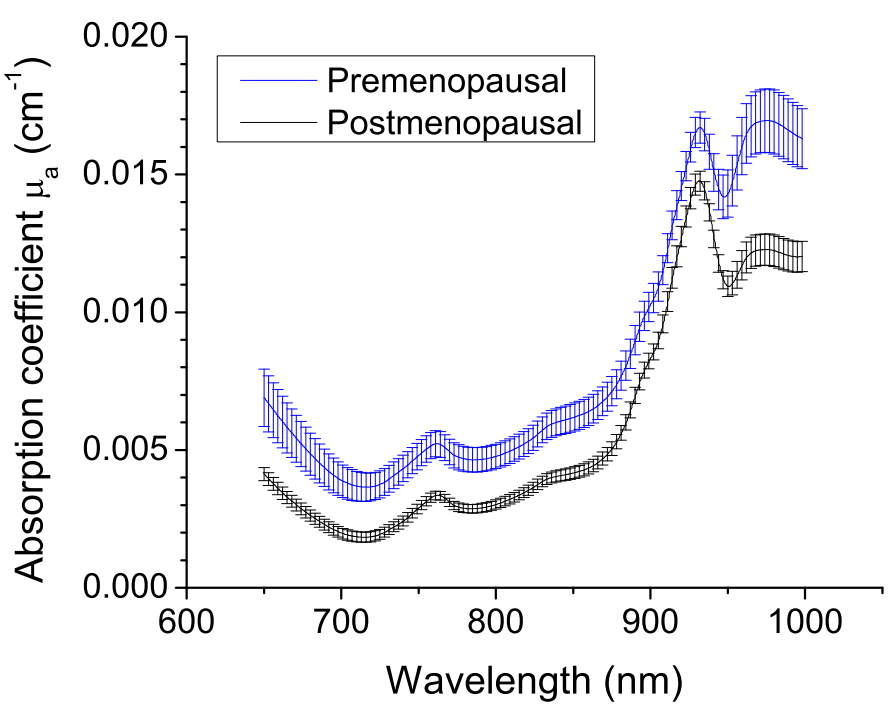
Premenopausal
Postmenopausal
Absorption coefficient μ_a (cm^{-1})
0.020
0.015
0.010
0.005
0.000
600
700
800
900
1000
Wavelength (nm)

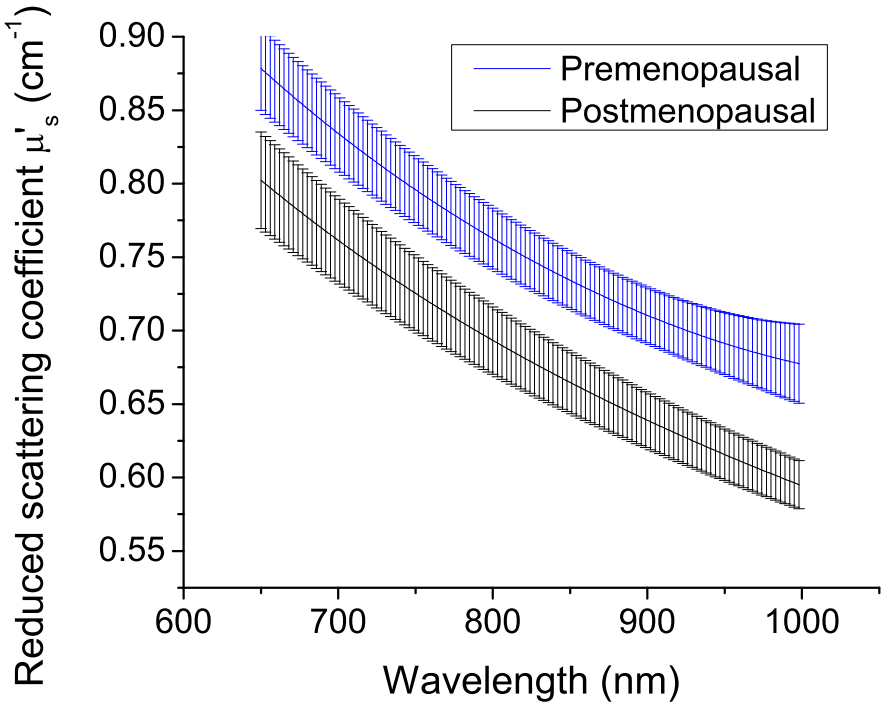
Premenopausal
Postmenopausal
Reduced scattering coefficient μ'_s (cm^{-1})
0.90
0.85
0.80
0.75
0.70
0.65
0.60
0.55
600
700
800
900
1000
Wavelength (nm)

Figure 2

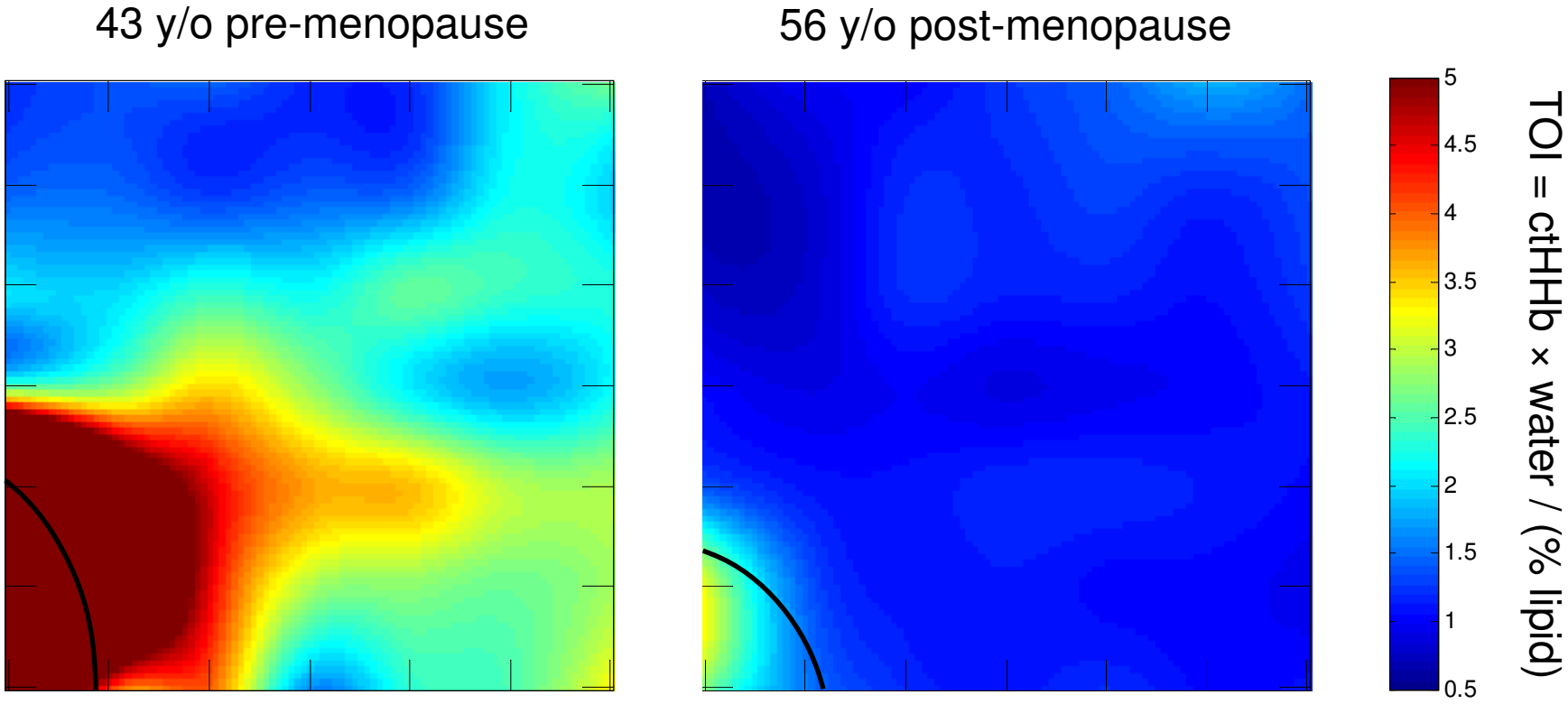
43 y/o pre-menopause
56 y/o post-menopause
5
4.5
4
3.5
3
2.5
2
1.5
1
0.5
TOI = ctHHb × water / (% lipid)

Figure 3

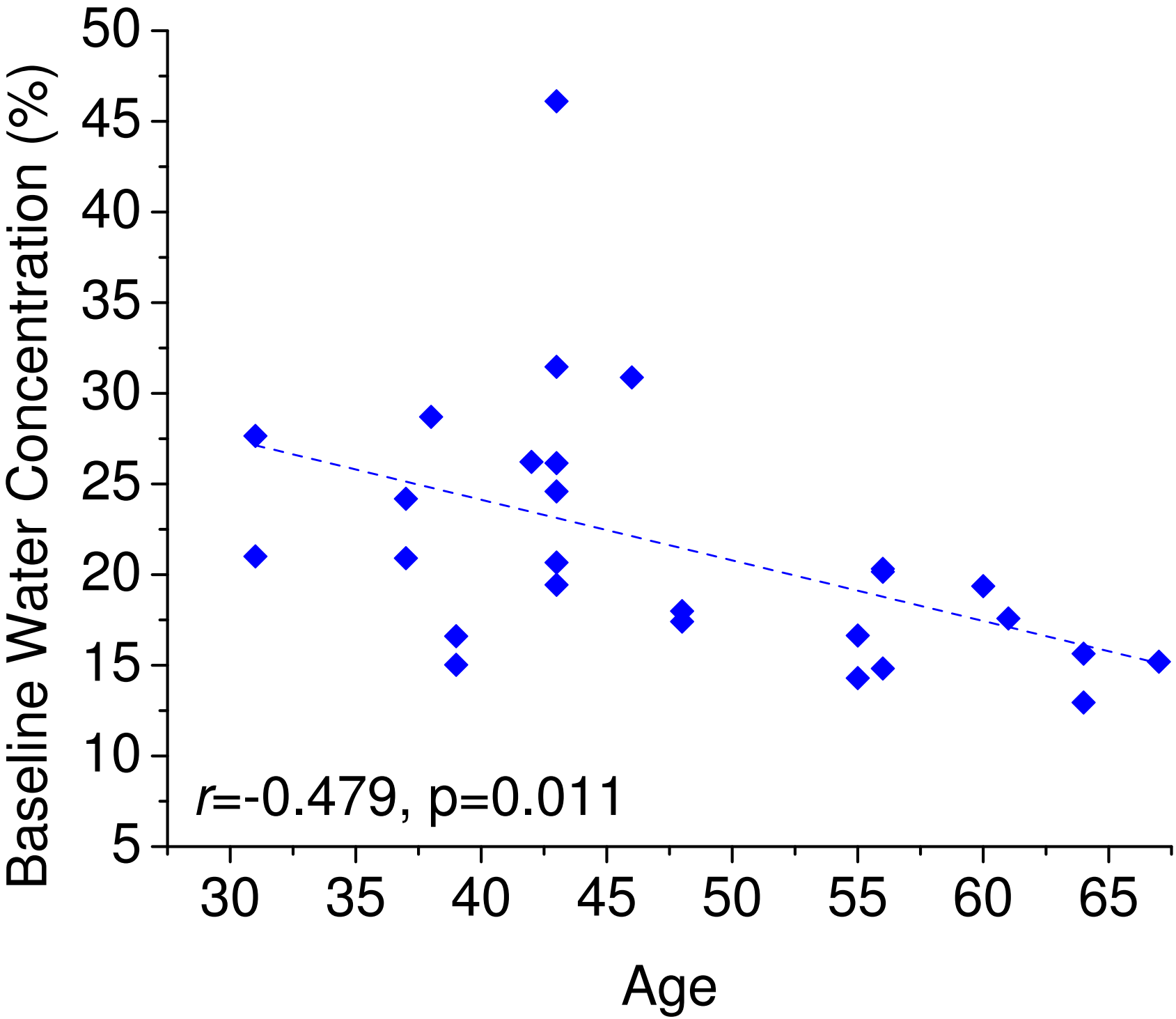
Baseline Water Concentration (%)
50
45
40
35
30
25
20
15
10
5
30
35
40
45
50
55
60
65
Age
r=-0.479, p=0.011

Figure 4

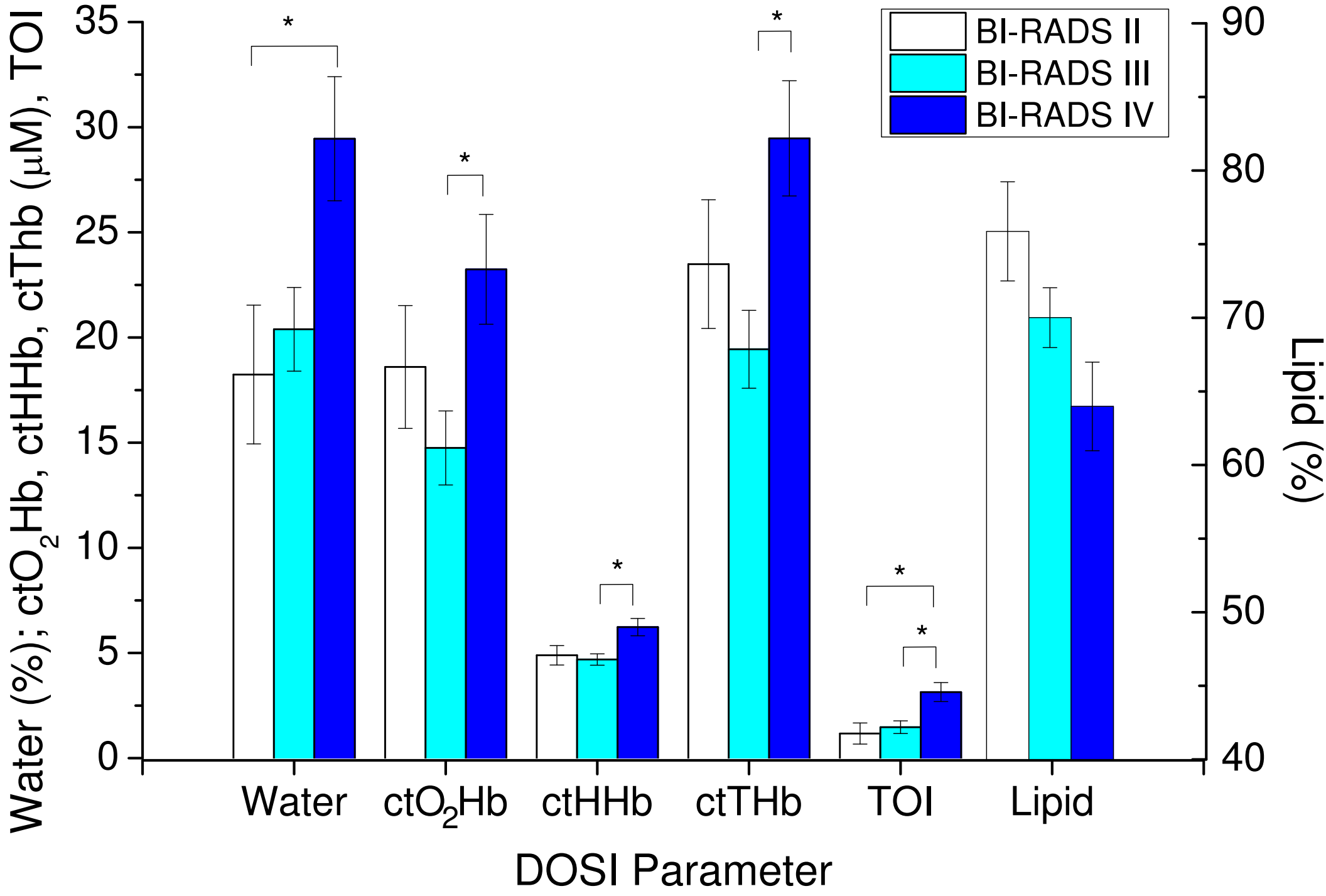
BI-RADS II
BI-RADS III
BI-RADS IV
Water (%); ctO2Hb, ctHHb, ctThb (μM), TOI
Lipid (%)
DOSI Parameter
Water
ctO2Hb
ctHHb
ctTHb
TOI
Lipid
0
5
10
15
20
25
30
35
40
50
60
70
80
90
*

Figure 5

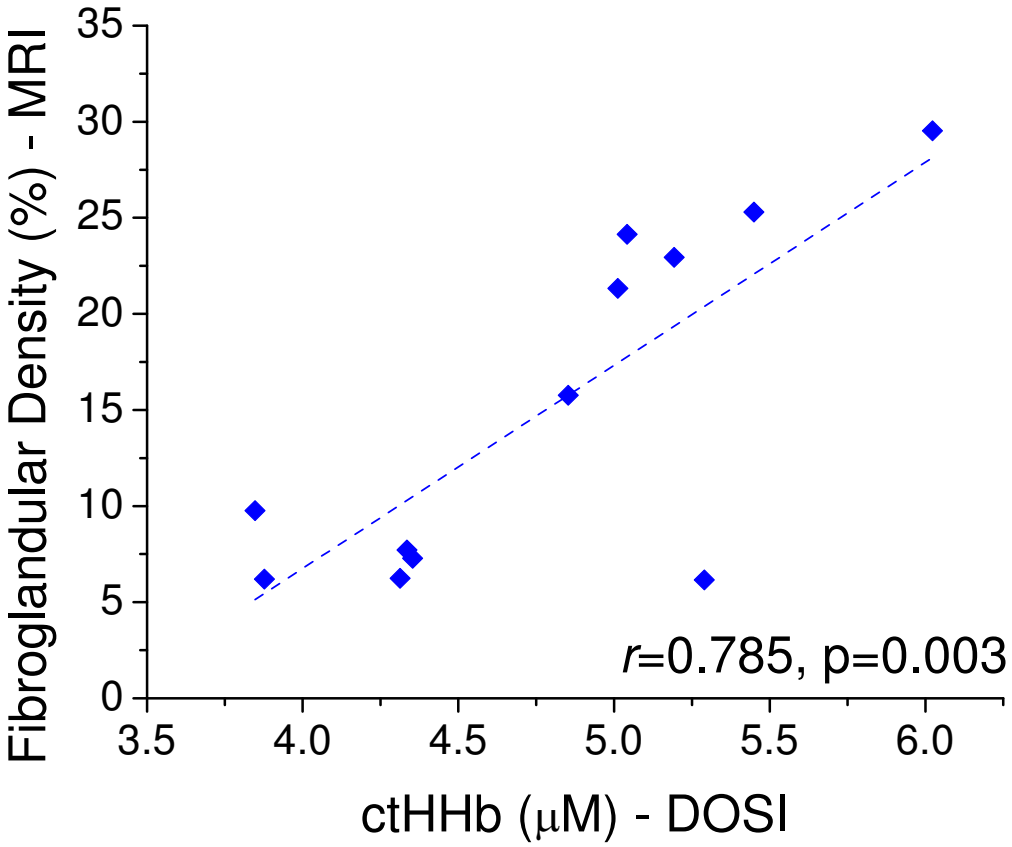
Fibroglandular Density (%) - MRI
ctHHb (μM) - DOSI
r=0.785, p=0.003
0
5
10
15
20
25
30
35
3.5
4.0
4.5
5.0
5.5
6.0

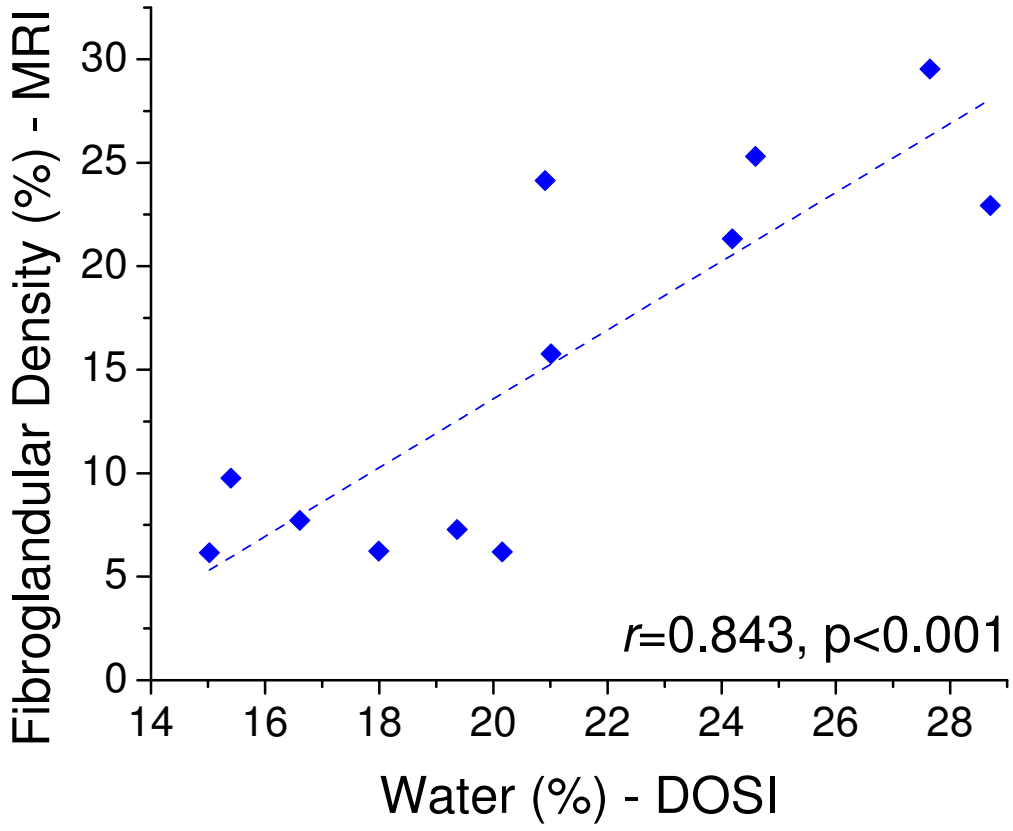
Fibroglandular Density (%) - MRI
Water (%) - DOSI
r=0.843, p<0.001
0
5
10
15
20
25
30
14
16
18
20
22
24
26
28

Figure 6

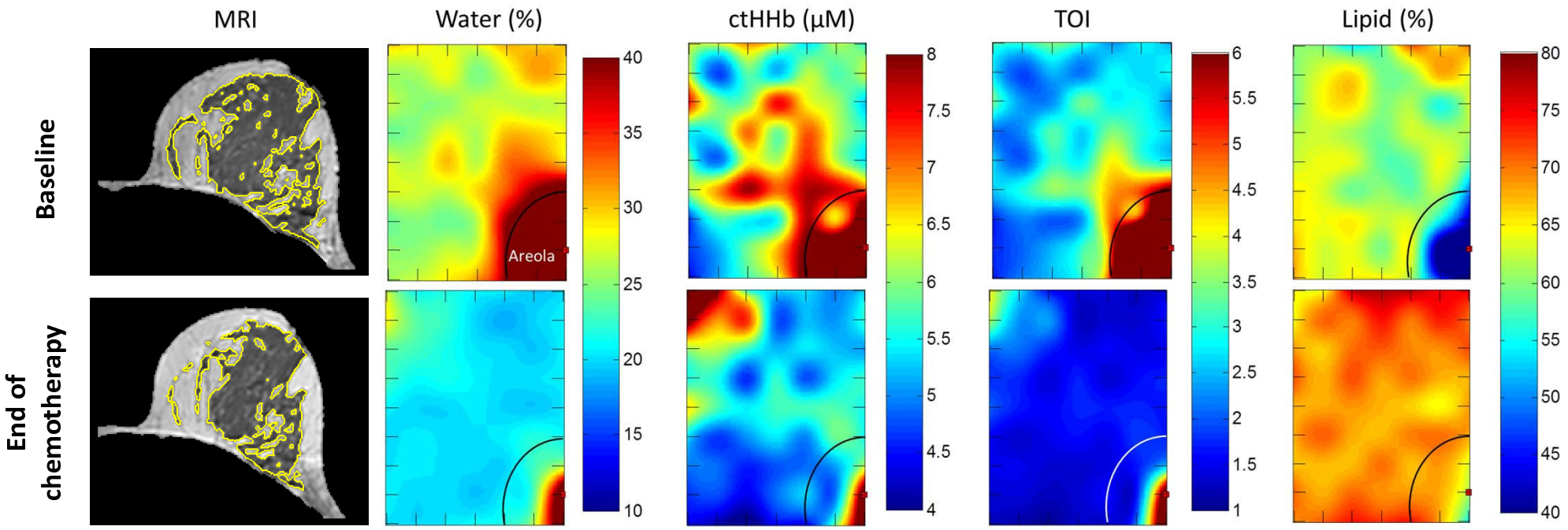
MRI
Water (%)
ctHHb (µM)
TOI
Lipid (%)
Baseline
End of chemotherapy
Areola
40
35
30
25
20
15
10
8
7.5
7
6.5
6
5.5
5
4.5
4
6
5.5
5
4.5
4
3.5
3
2.5
2
1.5
1
80
75
70
65
60
55
50
45
40

Figure 7

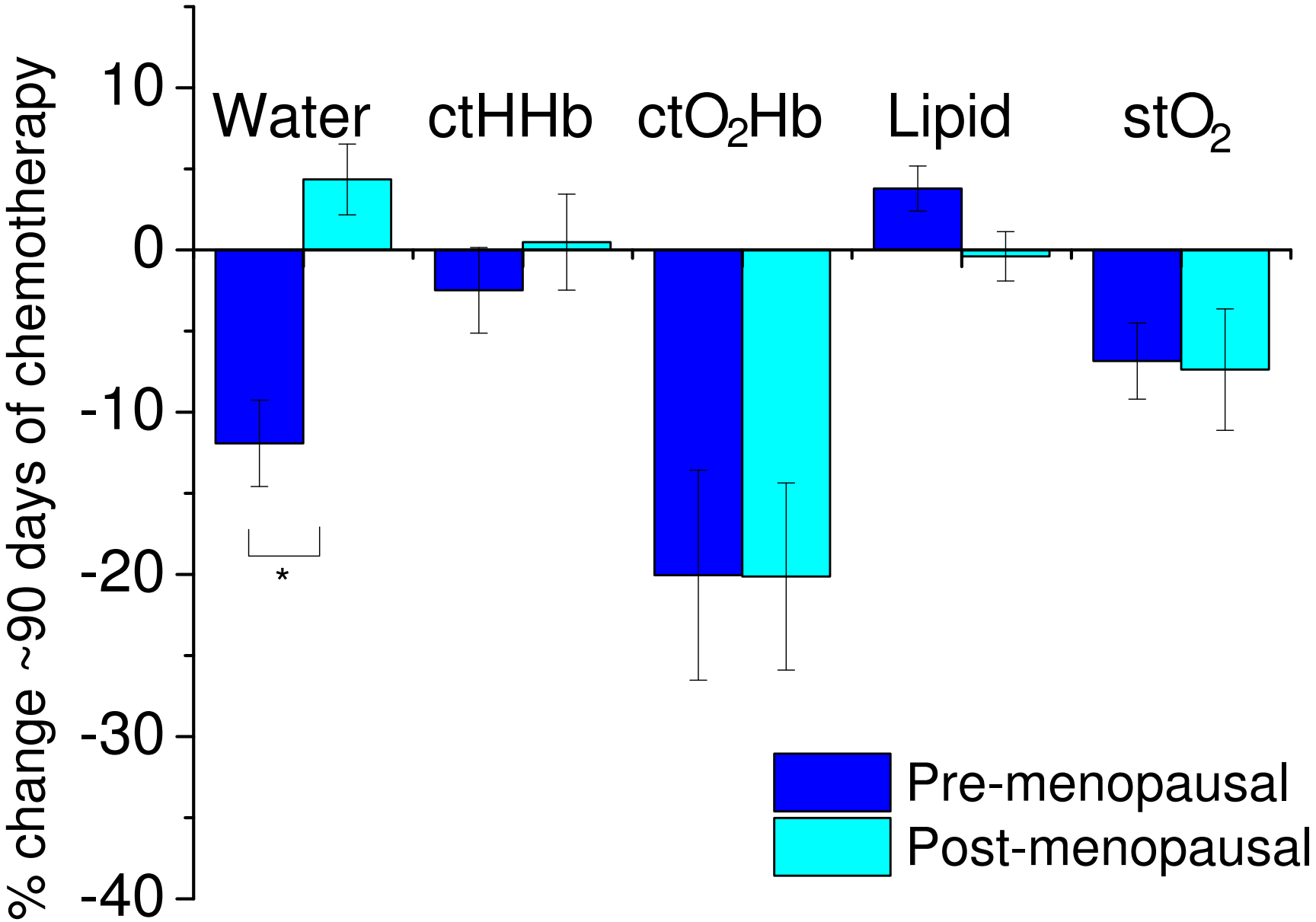
% change ~90 days of chemotherapy
10
0
-10
-20
-30
-40
Water
ctHHb
ctO2Hb
Lipid
stO2
*
Pre-menopausal
Post-menopausal

Figure 8

A

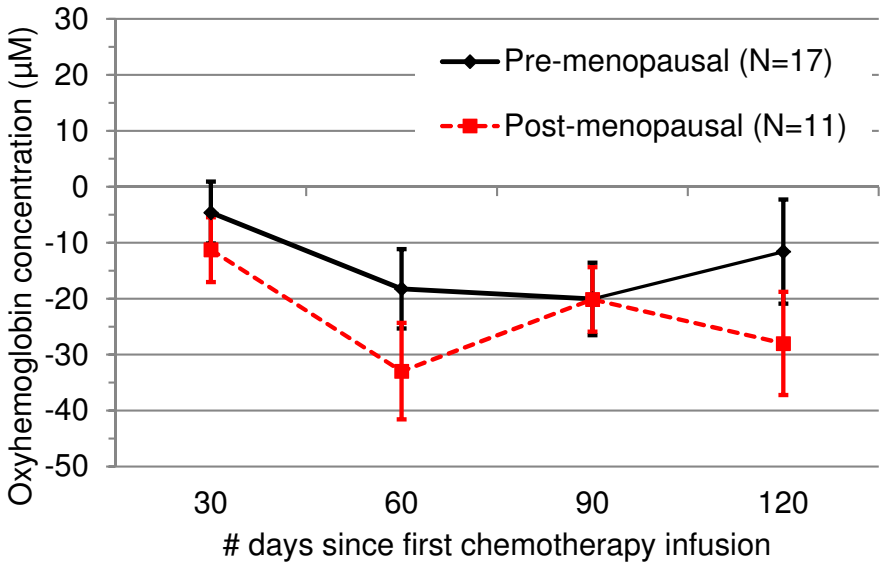
Oxyhemoglobin concentration (μM)
30
20
10
0
-10
-20
-30
-40
-50
Pre-menopausal (N=17)
Post-menopausal (N=11)
30
60
90
120
days since first chemotherapy infusion

B

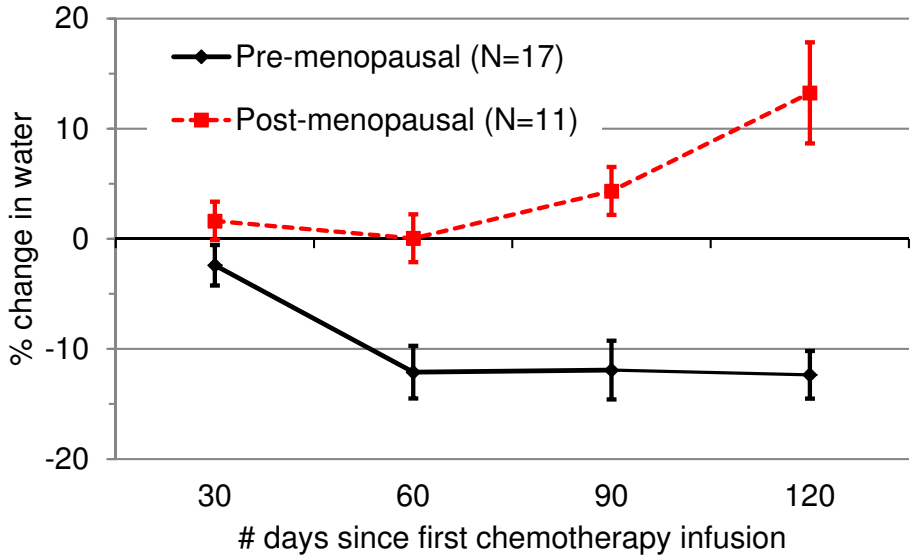
% change in water
20
10
0
-10
-20
Pre-menopausal (N=17)
Post-menopausal (N=11)
30
60
90
120
days since first chemotherapy infusion

C

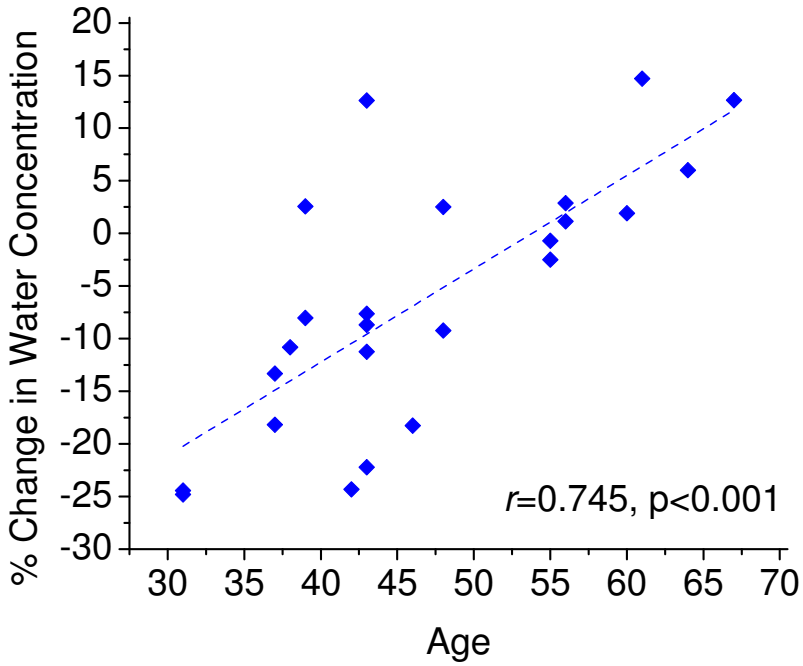
% Change in Water Concentration
20
15
10
5
0
-5
-10
-15
-20
-25
-30
r=0.745, p<0.001
30
35
40
45
50
55
60
65
70
Age

Figure 9

Additional files provided with this submission:

Additional file 1: Additional file 1.doc, 37K
http://breast-cancer-research.com/imedia/2062092005922576/supp1.doc
Additional file 2: Additional file 2.doc, 54K
http://breast-cancer-research.com/imedia/1679030229225766/supp2.doc